Precision *W*-boson and top-quark mass determinations at a muon collider

V. Barger,[1] M. S. Berger,[2] J. F. Gunion,[3] and T. Han[3]
[1]*Physics Department, University of Wisconsin, Madison, Wisconsin 53706*
[2]*Physics Department, Indiana University, Bloomington, Indiana 47405*
[3]*Physics Department, University of California, Davis, California 95616*
(Received 18 February 1997)

Precise determinations of the masses of the W boson and of the top quark could stringently test the radiative structure of the standard model (SM) or provide evidence for new physics. We analyze the excellent prospects at a muon collider for measuring M_W and m_t in the W^+W^- and $t\bar{t}$ threshold regions. With an integrated luminosity of 10 (100) fb^{-1}, the W-boson mass could be measured to a precision of 20 (6) MeV, and the top-quark mass to a precision of 200 (70) MeV, provided that theoretical and experimental systematics are understood. A measurement of $\Delta m_t = 200$ MeV for fixed M_W would constrain a 100 GeV SM Higgs boson mass within about ± 2 GeV, while $\Delta M_W = 6$ MeV for fixed m_t would constrain m_h to about ± 10 GeV. [S0556-2821(97)02615-5]

PACS number(s): 14.70.Fm, 07.77.Ka, 14.65.Ha

I. INTRODUCTION

Muon colliders offer a wide range of opportunities for exploring physics within and beyond the standard model (SM) [1–5]. An important potential application of these machines is the precision measurement of particle masses, widths, and couplings. Because the muon mass is much larger than the electron mass, initial state radiation from muons is substantially reduced compared to that from electrons and higher precision is possible in measuring cross sections in threshold regions. In this paper, we estimate the accuracy with which the W and t masses can be determined from W^+W^- and $t\bar{t}$ threshold measurements at a muon collider. We find that a muon collider with high luminosity may achieve greater accuracy for M_W and m_t than that by any other accelerator.

The W and Z masses are related by the equation

$$M_W = M_Z\left[1 - \frac{\pi\alpha}{\sqrt{2}G_\mu M_W^2(1-\delta r)}\right]^{1/2}, \tag{1}$$

where δr represents loop effects [6]. In the SM, δr depends quadratically on the top-quark mass and logarithmically on the Higgs boson mass (m_h). In the supersymmetric SM, δr may in addition depend on the masses of light supersymmetric particles, such as the chargino and top squark. The W and t mass errors should have a relative precision of

$$\Delta M_W \sim 0.7\times 10^{-2}\Delta m_t \tag{2}$$

in order that they lead to equivalent error in testing Eq. (1). The present world averages [7] for the W-boson mass and the top-quark mass are

$$M_W = 80.356 \pm 0.125 \text{ GeV}, \quad m_t = 175 \pm 6 \text{ GeV}, \tag{3}$$

for which $\Delta M_W/\Delta m_t \sim 2\times 10^{-2}$.

With high precision measurements of M_Z, M_W, and m_t, the consistency of the SM loop corrections can be tested and used to infer the Higgs boson mass through δr in Eq. (1). Figure 1 shows SM predictions of M_W (on-shell mass definition [8]) versus m_t for $m_h = 70$, 100, and 1000 GeV. With the present M_W and m_t measurements (the data point with error bars in Fig. 1), it is not yet possible to make a definitive distinction between the light Higgs boson ($m_h \sim 100$ GeV) and heavy Higgs boson ($m_h \sim 1$ TeV) scenarios. As future precision measurements narrow the allowed Higgs boson mass range, the results can be confronted with search limits or direct measurements of the Higgs boson mass.

The widths of the bands in Fig. 1 are due to the present uncertainties in the electromagnetic fine structure constant [9] and in the strong coupling constant [10]

$$\alpha^{-1}(M_Z) = 128.99 \pm 0.06, \quad \alpha_s(M_Z) = 0.118 \pm 0.005. \tag{4}$$

These errors in $\alpha^{-1}(M_Z)$ and in $\alpha_s(M_Z)$ translate into uncertainties on M_W of order 20 MeV and 4 MeV, respectively. Thus, an improvement in the uncertainty in the fine structure

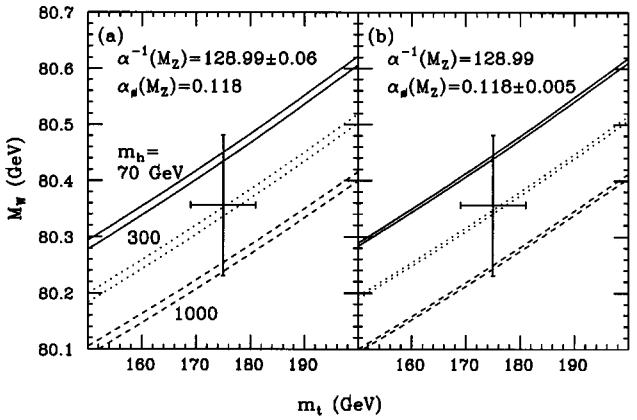

FIG. 1. Correlation between M_W and m_t in the SM with QCD and electroweak corrections [8] for $m_h = 70$, 300, and 1000 GeV. The data point and error bars are for $M_W = 80.356 \pm 0.125$ GeV and $m_t = 175 \pm 6$ GeV. The widths of the bands indicate the uncertainties (a) in $\alpha(M_Z)$ and (b) in $\alpha_s(M_Z)$.

constant at the Z mass scale will be needed to fully utilize a very accurate determination of M_W. The uncertainty in $\alpha^{-1}(M_Z)$ is due to measurement errors in the cross section for $e^+e^-\to$hadrons. The determination of $\alpha^{-1}(M_Z)$ given in Eq. (4) used the perturbative QCD cross section to fix the overall renormalization at c.m. energies above 6.5 GeV and for the nonresonant contributions in the region 3–3.9 GeV. Half of the uncertainty in $\alpha^{-1}(M_Z)$ in Eq. (4) is then due to the 1–2.5 GeV region and the other half due to the 2.5–5 GeV region. Calculations of $\alpha^{-1}(M_Z)$ have been made by other authors [11] without the use of perturbative QCD parametrization where the data are available. The cross section in the 1–5 GeV energy range for $e^+e^-\to$hadrons, now measured to 10% accuracy, could possibly be improved to 1% accuracy at the Beijing, Frascati, or Novosibirsk machines [9]. Measurements at this level of precision would translate into an overall error on $\alpha^{-1}(M_Z)$ of order ± 0.03 [12]. A 1% determination of $\alpha_s(M_Z)$ from future high energy experiments and lattice calculations is also anticipated [10].

Because of the importance of testing the radiative structure of the theory, it is appropriate to consider what improvements in precision measurements can be made at other colliders [13]. The planned upgrades of the Fermilab Tevatron collider will lead to improved M_W and m_t determinations through measurements of the $e\nu$ transverse mass and other techniques. With the Main Injector (MI, operational in 1999) and possible TeV33 upgrade, the anticipated precisions are [13]

$$\Delta M_W = 50 \pm 20 \text{ MeV}, \quad \Delta m_t = 4 \text{ GeV} \quad (2 \text{ fb}^{-1}, \text{ MI}), \tag{5}$$

$$\Delta M_W = 20 \text{ MeV}, \quad \Delta m_t = 2 \text{ GeV} \quad (10 \text{ fb}^{-1}, \text{ TeV33}). \tag{6}$$

At the CERN Large Hadron Collider (LHC), the expected accuracy for low-luminosity running is [13,14]

$$\Delta M_W = 15 \text{ MeV}, \quad \Delta m_t = 2 \text{ GeV} \quad (10 \text{ fb}^{-1}, \text{ LHC}). \tag{7}$$

Running the LHC at a higher luminosity (100 fb^{-1}/yr) is actually less effective for precision mass measurements due to the large background problem [14].

Experiments are currently underway at the CERN e^+e^- collider LEP 2 that will determine M_W by two methods [15]. The first is the measurement of the cross section at 161 GeV, just above the $2M_W$ threshold, to determine the mass via the SM prediction for the cross section. A precision of

$$\Delta M_W = 144 \text{ MeV} \quad (100 \text{ pb}^{-1}, \text{ LEP 2}) \tag{8}$$

is anticipated. This number assumes an integrated luminosity of 25 pb^{-1} in each of the four experiments. The second method is the reconstruction of the W mass in $W\to jj$ decay modes from $W^+W^-\to q\bar{q}q\bar{q}$ and $W^+W^-\to q\bar{q}\ell\nu$ final states at $\sqrt{s}=175$ GeV where the cross section is much larger. The achievable precision in this case is

$$\Delta M_W = 34 \text{ MeV} \quad (2 \text{ fb}^{-1}, \text{ LEP 2}). \tag{9}$$

At a Next Linear e^+e^- Collider (NLC), the anticipated precisions for M_W measurement [16] with $\sqrt{s}=500$ GeV and for m_t measurement [17] at the threshold $\sqrt{s}\sim 2m_t$ are

$$\Delta M_W = 20 \text{ MeV}, \quad \Delta m_t = 0.2 \text{ GeV} \quad (50 \text{ fb}^{-1}, \text{ NLC}), \tag{10}$$

where the M_W error is that for mass reconstruction in the $q\bar{q}$ decay mode. If the NLC energy is lowered to $\sqrt{s}=161$ GeV for a W^+W^- threshold determination of M_W, then scaling the statistical error of Eq. (8) implies $\Delta M_W \sim 20$ MeV (6 MeV) for an integrated luminosity of $L=5$ fb^{-1} (50 fb^{-1}), where the former is a rough estimate of the yearly luminosity that would result at $\sqrt{s}=161$ GeV for an interaction region designed for $L=50$ fb^{-1} per year at $\sqrt{s}=500$ GeV. The actual NLC errors would be larger, however, since systematic uncertainty in the central beam energy value as well as the beam energy spread would cause significant deterioration; detailed estimates are not available. In this paper, we show that such problems are minimal at a muon collider: an accuracy for M_W near the statistical level is possible and the accuracy on m_t would also be higher than that at the NLC. For an integrated luminosity of 50 fb^{-1}, we find that $\Delta M_W \sim 9$ MeV and $\Delta m_t \sim 100$ MeV can be achieved at a muon collider provided experimental systematic errors in cross section ratios related to detection efficiencies and certain theoretical systematic errors are sufficiently small.

The prospects for measuring the W boson mass at a muon collider were examined previously by Dawson [18], who concentrated on the case where only 100 pb^{-1} luminosity was available for the measurement. In this paper, we assume that the muon collider ring is optimized for the W threshold study and that up to 100 fb^{-1} is available.[1] In this situation one must confront the systematic errors that may dominate over the statistical ones. We find rough agreement with the scaled statistical error in Ref. [18]. We consider the systematic errors and how to minimize them in Sec. II.

The outline of the remainder of the paper follows. In Sec. II, we examine the accuracy with which M_W can be determined using cross section measurements at a $\mu^+\mu^-$ collider near the W^+W^- threshold. Determining m_t via measurements near the $t\bar{t}$ threshold is discussed in Sec. III. In Sec. IV, we summarize our results and emphasize the constraints on the SM Higgs boson mass from the precision M_W and m_t measurements.

II. M_W MEASUREMENT AT THE $\mu^+\mu^-\to W^+W^-$ THRESHOLD

In lepton collider measurements of M_W through reconstruction of $W\to q\bar{q}$ decays, the hadronic calorimeter resolution determines the achievable precision. The $WW\to q\bar{q}\ell\nu$ final state is preferable to $WW\to 4$ jets to

[1]Since the storage rings would comprise a modest fraction of the overall collider costs [19], it should be possible to have separate rings optimized for the threshold energies and then high luminosities can be realized.

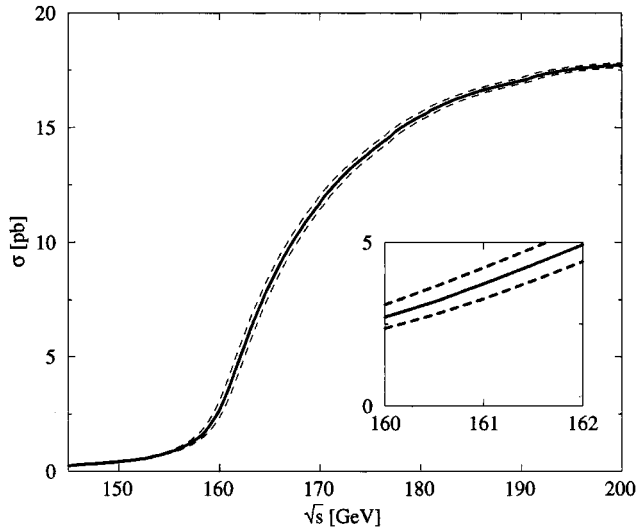

FIG. 2. The cross section for $\mu^+\mu^- \to W^+W^-$ in the threshold region for $M_W = 80.3$ GeV (solid) and $M_W = 80.1$, 80.5 GeV (dashed). The inlaid graph shows the region of the threshold curve where the statistical sensitivity to M_W is maximized. Effects of initial state radiation (ISR) have been included.

avoid potential uncertainties from the rescattering of quarks originating from different W bosons.

The alternative method of M_W determination based on accurate cross section measurement near the threshold is insensitive to the final state M_W reconstruction. A muon collider is particularly well suited to the threshold measurement because the energy of the beam has a very narrow spread. Thus, it is this approach that we concentrate on here.

The off-shell W^+W^- cross section that comprises the signal is

$$\sigma(s) = \int_0^s ds_1 \int_0^{(\sqrt{s}-\sqrt{s_1})^2} ds_2 \rho(s_1)\rho(s_2)\sigma_0(s,s_1,s_2) \times [1+\delta_C(s,s_1,s_2)], \tag{11}$$

where σ_0 is the Born cross section given in Ref. [20] and

$$\rho(s) = \frac{1}{\pi}\frac{\Gamma_W}{M_W}\frac{s}{(s-M_W^2)^2 + s^2\Gamma_W^2/M_W^2}. \tag{12}$$

The form for the Coulomb correction δ_C can be found in Ref. [21]. Initial state radiation (ISR) must also be included in the cross section calculation. Since the radiative effects are smaller for muons than for electrons, the signal cross section is slightly higher at a $\mu^+\mu^-$ collider. The predicted signal at a muon collider is plotted in Fig. 2 for several values of M_W.

The threshold cross section is most sensitive to M_W just above $\sqrt{s} = 2M_W$, but a tradeoff exists between maximizing the signal rate and the sensitivity of the cross section to M_W. Detailed analysis [15] shows that if the background level is small and systematic uncertainties in efficiencies are not important, then the optimal measurement of M_W is obtained by collecting data at a single energy

$$\sqrt{s} \sim 2M_W + 0.5 \text{ GeV} \sim 161 \text{ GeV},$$

where the threshold cross section is sharply rising.

For a LEP 2 measurement with 100 pb^{-1} of integrated luminosity the background and systematic uncertainties are, in fact, sufficiently small that the error for M_W will be limited by the statistical uncertainty of the measurement at $\sqrt{s} = 161$ GeV. But, at a muon collider or electron collider at high luminosity, systematic errors arising from uncertainties in the background level and the detection or triggering efficiencies will be dominant unless some of the luminosity is devoted to measuring the level of the background (which automatically includes somewhat similar efficiencies) at an energy below the W^+W^- threshold. Then, assuming that efficiencies for the background and W^+W^- signal are sufficiently well understood that systematic uncertainties effectively cancel in the ratio of the above-threshold to the below-threshold rates, a very accurate M_W determination becomes possible.

The dominant background derives from $e^+e^- \to (Z/\gamma)(Z/\gamma)$ which is essentially energy independent [15] below 180 GeV. For our present analysis we model the background as energy independent, and accordingly assume that one measurement at an energy in the range 140 to 150 GeV suffices to determine the background.

Thus, we analyze our ability to determine the W mass via just two measurements: one at center-of-mass energy $\sqrt{s} = 161$ GeV, just above threshold, and one at $\sqrt{s} = 150$ GeV. The signal is not entirely negligible at the lower energy (especially in the $q\bar{q}\ell\nu$ and $\ell\nu\ell\nu$ modes) due to off-shell W-decay contributions, but a two-parameter fit for M_W and the (constant) background can be made. The optimal M_W measurement is obtained by expending about two-thirds of the luminosity at $\sqrt{s} = 161$ GeV and one-third at $\sqrt{s} = 150$ GeV. We assume the signal detection efficiencies (not including branching fractions) of 55%, 47%, and 60% for the decay modes $WW \to q\bar{q}q\bar{q}, q\bar{q}\ell\nu, \ell\nu\ell\nu$, respectively, along with the background cross-section with cuts from Ref. [15].

Our joint determination of the signal (and hence the measurement of M_W) and background levels is shown in Fig. 3 for the mode $WW \to q\bar{q}q\bar{q}$. These results, for an integrated luminosity of 100 fb^{-1}, indicate that a determination of M_W to a precision of 9 MeV is possible in this final state, with the underlying background measured to 1% accuracy. Note that this 1% characterizes the level at which the systematic efficiency uncertainties must be under control in the ratio of the 161 and 150 GeV cross section measurements. The ± 9 MeV uncertainty for M_W is equivalent to about a 0.5% measurement of the signal cross section as apparent in Fig. 2, where the inset shows that a 200 MeV shift in M_W results in about a 10% shift in the cross section.

Table I lists the achievable M_W precision in the various W-decay modes for 100 fb^{-1} of integrated luminosity. Combining the three modes, an overall precision of

$$\Delta M_W = 6 \text{ MeV} \tag{13}$$

should be achievable. The above analysis assumes the predicted SM width Γ_W. An uncertainty in Γ_W may translate into an uncertainty in M_W since Γ_W can affect the cross section at the threshold. Quantitatively, the relation at

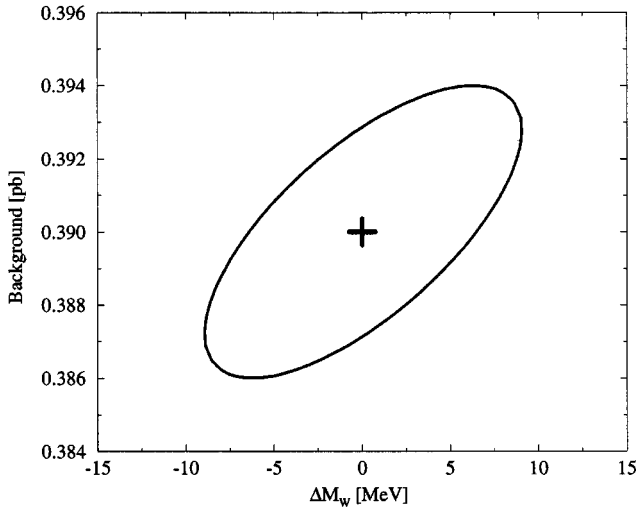

FIG. 3. A sample $\Delta\chi^2=1.0$ contour for the background and signal measurement in the W^+W^- threshold region for the final state $q\bar{q}q\bar{q}$ with an integrated luminosity of 100 fb^{-1}. Effects of ISR have been included. A central mass value $M_W=80.356$ GeV is assumed.

$\sqrt{s}=161$ GeV is[2] $\Delta M_W \simeq 0.17\Delta\Gamma_W$. The current experimental error $\Delta\Gamma_W \simeq 60$ MeV [22] thus translates into an uncertainty of $\Delta M_W \sim 10$ MeV. With a 10 fb^{-1} integrated luminosity at the Tevatron upgrade, $\Delta\Gamma_W \simeq 20$ MeV can be achieved [23], which translates into an uncertainty $\Delta M_W \sim 3$ MeV. It is interesting to note that there is essentially no dependence of the cross section on Γ_W near $\sqrt{s}=162$ GeV, so that the uncertainty due to $\Delta\Gamma_W$ can be minimized by performing the measurements at this energy without degrading the M_W determination.

Let us return to the issue of theoretical and experimental systematic uncertainties. On the theoretical side, there are uncertainties in M_W from mass definition schemes and the renormalization scale which may be on the order of a few MeV [8]. Therefore, careful theoretical consideration is required to extract the precise [e.g., modified minimal subtraction $(\overline{\mathrm{MS}})$] M_W value and test loop effects. Higher order corrections to the signal cross section remain to be evaluated, but such calculations are not a serious obstacle.

The largest systematic effects, however, may be those associated with the background treatment and systematic errors in the detection or triggering efficiencies. First, a more refined treatment of the energy dependence of the background may prove to be necessary. Theoretical calculations can be used to input the energy dependence and be checked via measurements made at more than one subthreshold energy. Excellent accuracy on the energy dependence should be possible. The biggest uncertainty is likely to arise from lack of knowledge of the efficiencies. In particular, the background and the signal are somewhat different in that the background has different leptonic modes and different percentages of jet-jet final states relative to leptonic final states. It will be crucial that the efficiency for background final states relative to that for signal final states be understood to better than the 1% level. Alternatively, the technique of determining M_W by measuring the W^+W^- signal well above threshold, $\sqrt{s}\gtrsim 200$ GeV, and taking the ratio to the $\sqrt{s}=161$ GeV measurement could also be considered, since the final states involved are the same, and efficiencies for detection or triggering may cancel to the needed degree of accuracy.

TABLE I. Signal and background cross sections for $\mu^+\mu^-\to W^+W^-$ and the achievable precision in M_W with 100 fb^{-1} luminosity. A central mass value $M_W=80.356$ GeV is assumed.

	$q\bar{q}q\bar{q}$	$q\bar{q}\ell\nu$	$\ell\nu\ell\nu$
Signal [pb] at $\sqrt{s}=161$ GeV	0.97	0.77	0.25
Signal [pb] at $\sqrt{s}=150$ GeV	0.11	0.086	0.028
Background [pb]	0.39	0.03	0.01
ΔM_W [MeV]	9	8	14

Uncertainty in M_W due to uncertainty in the beam energy is roughly given by $\Delta M_W \simeq \Delta E_{\mathrm{beam}}$ [15]. At a muon collider $\Delta E_{\mathrm{beam}} < 10^{-5} E_{\mathrm{beam}}$ is achievable [19], implying $\Delta M_W \leqslant 0.8$ MeV. Beam energy smearing will also have negligible impact on M_W so long as the Gaussian width is known and is much less than Γ_W. Finally, the relative luminosity at $\sqrt{s}=150$ GeV and 161 GeV must be known to better than 0.5% for the systematic error from this source to yield $\Delta M_W < 6$ MeV.

III. TOP-QUARK MASS MEASUREMENT AT THE $\mu^+\mu^-\to t\bar{t}$ THRESHOLD

There is very rich physics associated with the $t\bar{t}$ threshold, including the determination of m_t, Γ_t ($|V_{tb}|$), α_s, and possibly m_h [24]. A precise value of the top-quark mass m_t could prove to be very valuable in theoretical studies. For example, if a particle desert exists up to the grand unified theory scale, we will want to extrapolate from low energy to the grand unified scale to probe in a detailed way the physics at the unification scale. The top-quark mass (and its Yukawa coupling) are crucially important since they determine to a large extent the evolution of all the other Yukawa couplings, including flavor mixings. If the top-quark Yukawa coupling is determined by an infrared quasifixed point [25], very small changes in m_t translate into very large changes in the renormalized values of many other parameters in the theory.

Fadin and Khoze first demonstrated that the top-quark threshold cross section is calculable since the large top-quark mass puts one in the perturbative regime of QCD, and the large top-quark width effectively screens nonperturbative effects in the final state [26]. Such studies have since been performed by several groups [27–34]. There are two equivalent ways to obtain the total cross section near threshold by solving for a three-point Green's function in either coordinate [29] or momentum space [30]. Here we solve Schrödinger's equation in coordinate space

$$\left[-\frac{\Delta}{m_t}+V(r)-\left(E+i\frac{\Gamma_\Theta}{2}\right)\right]G(\mathbf{x};E)=\delta^3(\mathbf{x}), \qquad (14)$$

[2]This is similar to the case at LEP 2 [15], even though the cross section dependence on M_W and Γ_W at a muon collider is stronger.

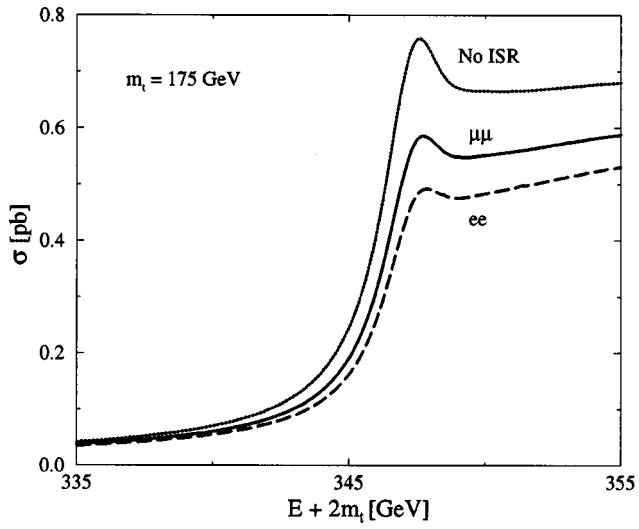

FIG. 4. The cross section for $t\bar{t}$ production at a lepton collider in the threshold region, for $m_t=175$ GeV and $\alpha_s(M_Z)=0.12$. The results for $\mu\mu$ and ee colliders include the effects of ISR (but no beam smearing), and the top curve does not.

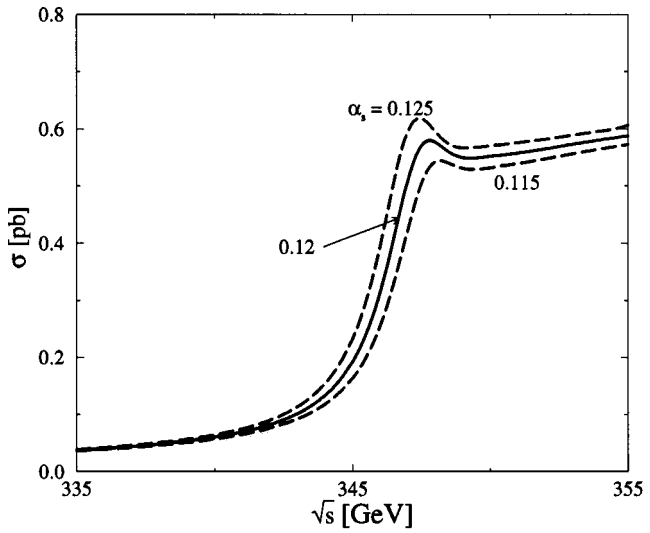

FIG. 5. The cross section for $\mu^+\mu^-\to t\bar{t}$ production in the threshold region, for $m_t=175$ GeV and $\alpha_s(M_Z)=0.12$ (solid) and 0.115, 0.125 (dashes). Effects of ISR and beam smearing are included.

where Γ_Θ is the (running) toponium width, and $E=\sqrt{s}-2m_t$. The potential $V(r)$ is given for small r by two-loop perturbative QCD and for large r by a fit to quarkonia spectra. In our analysis we make use of the Wisconsin potential [35] that interpolates these regimes. However, the short range part of the potential alone determines the physics at the top-quark threshold. The cross section is proportional to $\mathrm{Im}G(\mathbf{x}=0;E)$ with [29,34]

$$\sigma_{t\bar{t}}=\frac{96\pi^2\alpha^2}{s^2}\left\{1-\frac{16\alpha_s}{3\pi}\right\}[(Q_eQ_t+v_ev_t\chi)^2 +(a_e^2v_t^2\chi^2)]\mathrm{Im}G(\mathbf{x}=0;E=\sqrt{s}-2m_t), \quad (15)$$

where $\chi=s/(s-M_Z^2)$. The cross section depends on the strong gauge coupling $\alpha_s(M_Z)$ through the potential $V(r)$.

Figure 4 shows the calculated threshold curve for $\mu^+\mu^-$ or $e^+e^-\to t\bar{t}$ including the effects of ISR for a top-quark mass of 175 GeV. The initial state radiation causes a reduction of the cross section as well as a smearing of the small resonance peak. The effect is less severe for a muon collider (long dashed) than that for an e^+e^- collider (short dashed) due to the heavier muon mass.

The beam energy spread is the major experimental problem in precision measurements of the top-quark threshold region at an e^+e^- collider. Reference [31] demonstrated the effects of beam smearing for some proposed e^+e^- machine designs, and argued that a narrow beam was essential for studying the $t\bar{t}$ threshold region. A high resolution determination of the e^+e^- collider energy profile is desirable in order to be able to deconvolute the smearing of the threshold curve.

For a muon collider a measurement of the beam profile is unnecessary, since a very narrow beam is a natural characteristic. The rms deviation σ in $\sqrt{s}$ is given by [36,37]

$$\sigma=(250\ \mathrm{MeV})\left(\frac{R}{0.1\%}\right)\left(\sqrt{\frac{s}{360\ \mathrm{GeV}}}\right), \quad (16)$$

where R is the rms deviation of the Gaussian beam profile. With $R\lesssim 0.1\%$ the resolution σ is of the same order as the measurement one hopes to make in the top-quark mass. For $t\bar{t}$ studies the exact shape of the beam is not important if $R\lesssim 0.1\%$. We take $R=0.1\%$ here; the results are not improved significantly with better resolution.

Changing the value of the strong coupling constant $\alpha_s(M_Z)$ influences the threshold region. Large values lead to tighter binding and the peak shifts to lower values of $\sqrt{s}$. Weaker coupling also smooths out the threshold peak. These effects are illustrated in Fig. 5.

To assess the precision of parameter determinations from cross section measurements, we generate hypothetical sample data, shown in Fig. 6, assuming that 10 fb^{-1} integrated luminosity is used to measure the cross section at each energy in 1 GeV intervals. Since the top-quark threshold curve depends on other quantities such as $\alpha_s(M_Z)$, one must do a full scan to determine the shape of the curve and its overall normalization. To generate the ten data points in Fig. 6 we use nominal values of $m_t=175$ GeV and $\alpha_s(M_Z)=0.12$. Following Ref. [34], we assume a 29% detection efficiency for $W\to q\bar{q}$, including the decay branching fraction. The data points can then be fit to theoretical predictions for different values of m_t and $\alpha_s(M_Z)$; the likelihood fit that is obtained is shown as the $\Delta\chi^2$ contour plot in Fig. 7. The inner and outer curves are the $\Delta\chi^2=1.0$ (68.3%) and 4.0 (95.4%) confidence levels, respectively, for the full 100 fb^{-1} integrated luminosity. Projecting the $\Delta\chi^2=1.0$ ellipse on the m_t axis, the top-quark mass can be determined to within $\Delta m_t\sim 70$ MeV, provided systematics are under control. (Systematic error issues will be discussed later.) A top-quark mass of 175 GeV can be measured to about 200 MeV at 90% confidence level with 10 fb^{-1} luminosity. This is about a factor of 1.7 better in Δm_t than the same measurement at an e^+e^- machine when realistic beam effects are included [34].

Since the exchange of a light Higgs boson can affect the threshold shape, a scan of the threshold cross section can in

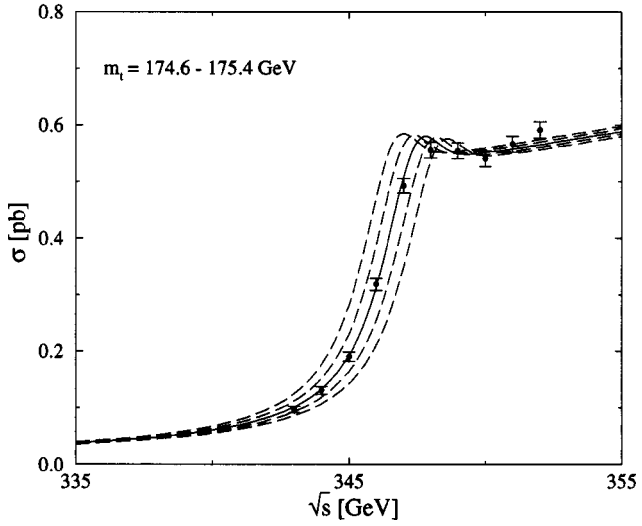

FIG. 6. Sample data for $\mu^+\mu^- \to t\bar{t}$ obtained assuming a scan over the threshold region devoting 10 fb^{-1} luminosity to each data point. A detection efficiency of 29% has been assumed [34] in obtaining the error bars. The threshold curves correspond to shifts in m_t of 200 MeV increments. Effects of ISR and beam smearing have been included, and the strong coupling $\alpha_s(M_Z)$ is taken to be 0.12.

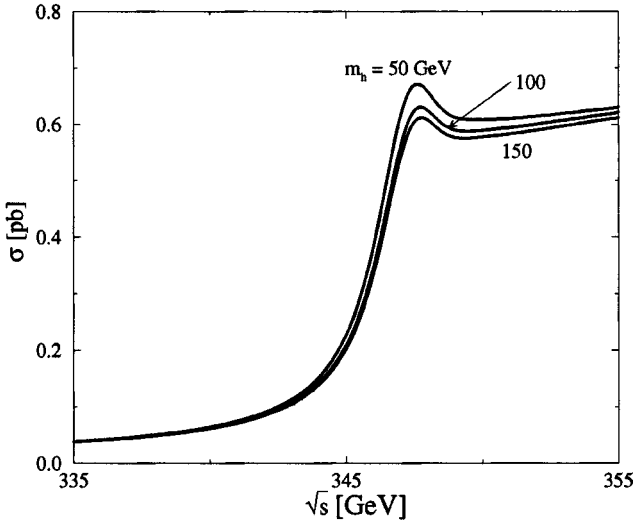

FIG. 8. The dependence of the threshold region on the Higgs boson mass, for $m_h = 50$, 100, 150 GeV. Effects of ISR and beam smearing have been included, and we have assumed $m_t = 175$ GeV and $\alpha_s(M_Z) = 0.12$.

principle yield some information about the Higgs boson mass and its Yukawa coupling to the top quark. Figure 8 shows the dependence of the threshold curve on the Higgs boson mass m_h. The effect of the Higgs boson vertex correction can be obtained [38] by including a Yukawa interaction in the QCD potential,

$$V_h(r) = -\sqrt{\frac{2G_F}{4\pi r}} m_t^2 e^{-m_h r}, \tag{17}$$

which effectively results in multiplying the resulting cross section by a small energy-independent correction factor.[3] However, it may be difficult to disentangle such a Higgs effect from two-loop QCD effects, which are not yet fully calculated [40].

In addition to the Higgs Yukawa potential effect, there is an additional *s*-channel Higgs boson contribution [36,37] to the cross section at a muon collider since the muon has a larger Yukawa coupling than does the electron; however, the *s*-channel contribution is much smaller than the usual photon and *Z* exchanges considered here.

Changing the top-quark width from its value in the standard model also affects the threshold shape. The width can be parametrized in terms of the CKM element $|V_{tb}|$, for which one expects $|V_{tb}| \approx 1$ in the standard model. A value $|V_{tb}| > 1$ would indicate new physics contribution to the top-quark decay, such as $t \to bH^+$. The dependence on $|V_{tb}|^2$ is shown in Fig. 9. A narrower top quark (smaller $|V_{tb}|$) results in a more prominent 1*S* peak in the cross section.

It should be possible to experimentally distinguish the various effects on the $t\bar{t}$ threshold shape. In Fig. 10 we show the dependence of four quantities

$$\begin{aligned} &\text{(a)}\ [\sigma(\text{peak}) - \sigma(340)]/\sigma(340), \\ &\text{(b)}\ [\sigma(350) - \sigma(340)]/\sigma(340), \\ &\text{(c)}\ [\sigma(\text{peak}) - \sigma(350)]/\sigma(350), \\ &\text{(d)}\ \sqrt{s}_{\text{peak}}, \end{aligned} \tag{18}$$

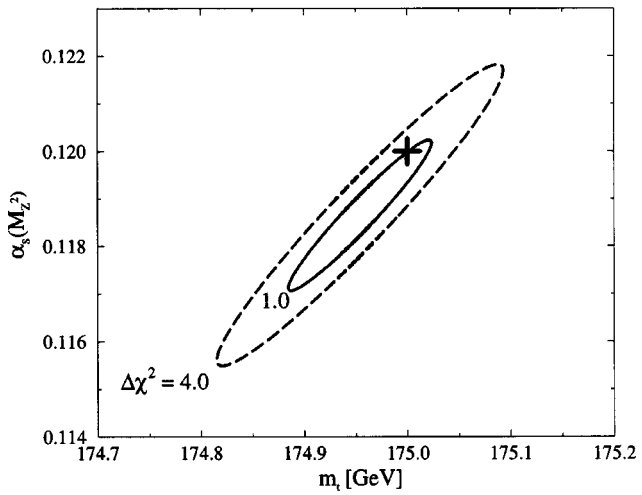

FIG. 7. The $\Delta\chi^2 = 1.0$ and $\Delta\chi^2 = 4.0$ confidence limits for the sample data shown in Fig. 6. The ''+'' marks the input values from which the data were generated.

[3]Equation (17) assumes the SM Higgs boson to $t\bar{t}$ coupling. In the case of the minimal supersymmetric model, the couplings of the lightest Higgs boson *h* become very similar to those of the SM Higgs boson in the large m_A limit (where *A* is the *CP*-odd neutral Higgs boson) [39].

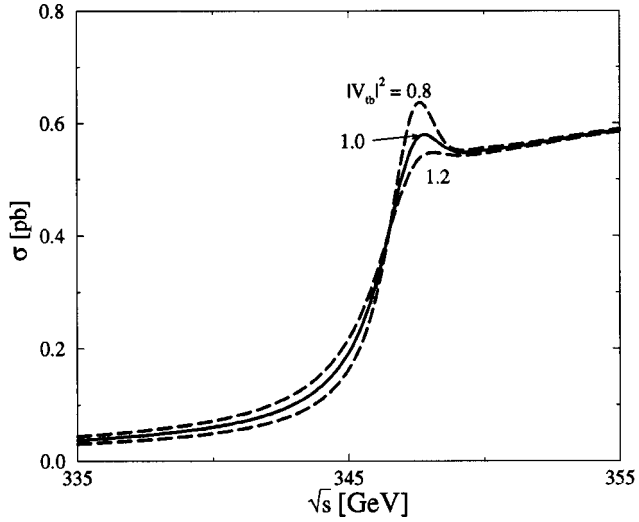

FIG. 9. The dependence of the threshold region for $\mu^+\mu^- \to t\bar{t}$ production on the $|V_{tb}|^2 = 0.8, 1.0, 1.2$. Effects of ISR and beam smearing have been included, and we have assumed $m_t = 175$ GeV and $\alpha_s(M_Z) = 0.12$.

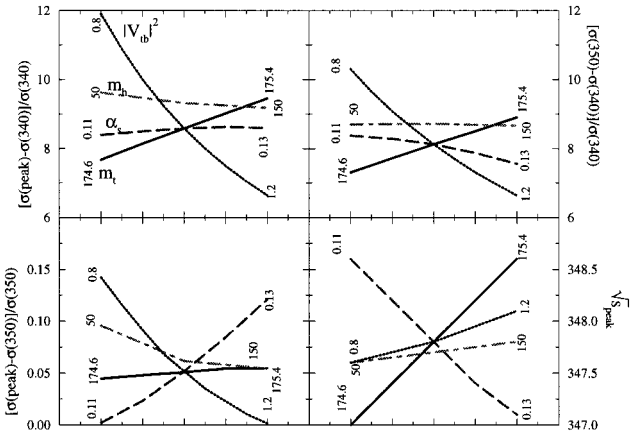

FIG. 10. The dependence of various measurable ratios on m_t, α_s, m_h, and $|V_{tb}|^2$. The Higgs Yukawa potential of Eq. (17) is only included in the m_h curves.

on the parameters m_t, α_s, m_h, and $|V_{tb}|$. Here $\sqrt{s}_{\rm peak}$ is the c.m. energy of the peak in the cross section and $\sqrt{s} = 340$ and 350 GeV are energies above and below this peak. These four quantities show different dependencies on the four parameters; consequently, detailed fits to threshold data should determine the parameters. In Fig. 10, the central values of $m_t = 175$ GeV, $\alpha_s = 0.12$, and $|V_{tb}|^2 = 1.0$ were chosen and then one parameter was varied to make the corresponding curve. The m_h curves show the effect of including a Higgs Yukawa contribution to the potential.

Additional information can be obtained by measuring the top-quark momentum from a reconstruction of the decay [34], providing further constraints on α_s and $|V_{tb}|$ (the dependence on m_t is small).

We now consider a variety of systematic uncertainties and/or issues.

QCD measurements at future colliders and lattice calculations will presumably determine $\alpha_s(M_Z)$ to 1% accuracy (e.g., ± 0.001) [10] by the time muon colliders are constructed so the uncertainty in α_s will likely be similar to the precision obtainable at a $\mu^+\mu^-$ and/or e^+e^- collider with 100 fb^{-1} integrated luminosity. If the luminosity available for the threshold measurement is significantly less than 100 fb^{-1}, one can regard the value of $\alpha_s(M_Z)$ coming from other sources as an input, and thereby improve the top-quark mass determination.

There is some theoretical ambiguity in the mass definition of the top quark. The theoretical uncertainty on the quark pole mass due to QCD confinement effects is of order $\Lambda_{\rm QCD}$, i.e., a few hundred MeV [41]. In the $\overline{\rm MS}$ scheme of quark mass definition, the theoretical uncertainty is better controlled.

Systematic errors in experimental efficiencies are not a significant problem for the $t\bar{t}$ threshold determination of m_t. This can be seen from Fig. 6, which shows that a 200 MeV shift in m_t corresponds to nearly a 10% shift in the cross section on the steeply rising part of the threshold scan, whereas it results in almost no change in σ once $\sqrt{s}$ is above the peak by a few GeV. Not only will efficiencies be known to much better than 10%, but also systematic uncertainties will cancel to a high level of accuracy in the ratio of the cross section measured above the peak to measurements on the steeply rising part of the threshold curve.

As Fig. 8 shows, it will be important to know the Higgs boson mass and the $ht\bar{t}$ coupling strength in order to eliminate this source of systematic uncertainty when extracting other quantities.

The measurements described in this section can be performed at either an e^+e^- or a $\mu^+\mu^-$ collider. The errors for m_t that we have found for the muon collider are smaller than those previously obtained in studies at the NLC electron collider primarily because the smearing of the threshold region by the energy spread of the beam is much less, and secondarily due to the fact that the reduced amount of initial state radiation makes the cross section somewhat larger.

IV. CONCLUSION

A muon collider offers an unparalleled opportunity for precision W- and top-quark mass measurements in the respective threshold regions. Table II compares the precision

TABLE II. Comparison for the achievable precision in M_W and m_t measurement at different future colliders.

	LEP 2		Tevatron		LHC	NLC	$\mu^+\mu^-$	
$\mathcal{L}$ (fb^{-1})	0.1	2	2	10	10	50	10	100
ΔM_W (MeV)	144	34	35	20	15	20	20	6
Δm_t (GeV)	–	–	4	2	2	0.2	0.2	0.07

achievable for M_W and m_t at present and future colliders.

We summarize our main results as follows.

At the W threshold, the optimum strategy is to expend about 2/3 of the luminosity at $\sqrt{s}=161$ GeV, just above $2M_W$, and about 1/3 at $\sqrt{s}=150$ GeV to measure the background and normalize efficiencies. With 10 (100) fb^{-1} of integrated luminosity at a muon collider, M_W could be measured to a precision of 20 (6) MeV, provided that the theoretical cross sections for the W^+W^- signal are evaluated to the $\lesssim O(1\%)$ level and that no irreducible systematic (in particular, experimental errors for cross section ratios) remains at this level.

With an integrated luminosity of 10 (100) fb^{-1}, the top-quark mass can be measured to 200 (70) MeV, using a ten-point scan over the threshold region, in 1 GeV intervals, to measure the shape predicted by the QCD potential. In the $t\bar{t}$ threshold study, differences of cross sections at energies below, at, and above the resonance peak, along with the location of the resonance peak, have different dependencies on the parameters m_t, α_s, m_h, and $|V_{tb}|^2$ and should allow their determination. To utilize the highest precision measurements achievable at the statistical level, theoretical uncertainties and other systematics need to be under control. We are confident that uncertainty in α_s will not be a factor and we have noted that ratios of above-peak measurements to measurements on the steeply rising part of the threshold cross section will eliminate many experimental systematics related to uncertainties in efficiencies.

The combination of the measurements of the masses M_Z, M_W, and m_t to such high precision has dramatic implications for the indirect prediction of the mass of the Higgs boson and for other sources of physics beyond the standard model. This is illustrated in Fig. 11. Assuming the current central values of M_W, m_t, $\alpha(M_Z)$, and $\alpha_s(M_Z)$, and that $L=10$ fb^{-1} (100 fb^{-1}) is devoted to the measurement of m_t (M_W), the mass of the SM Higgs boson would be determined to be 260 GeV with an error of about ± 5 GeV from $\Delta m_t=200$ MeV at a fixed M_W, and about ± 20 GeV from $\Delta M_W=6$ MeV at a fixed m_t. For $m_h=100$ GeV, the corresponding values would be ± 2 GeV and ± 10 GeV, respectively. More generally, the Δm_h value scales roughly like m_h.

Concerning the indirect determination of m_h from the radiative correction relations, there is no need to devote more than 10 fb^{-1} of luminosity to determining m_t; indeed, the ideal ratio of Eq. (2) would be reached for just $L\sim 0.6$ fb^{-1} (yielding $\Delta m_t\sim 900$ MeV) if $\Delta M_W\sim 6$ MeV.

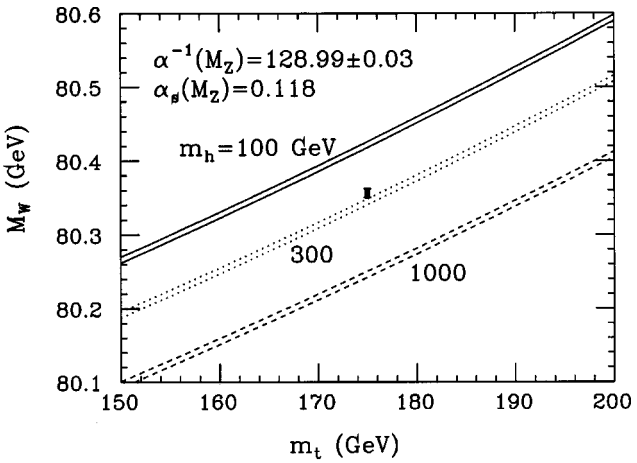

FIG. 11. Correlation between M_W and m_t in the SM with QCD and electroweak corrections for $m_h=100$, 300, and 1000 GeV. The data point and error bars illustrate the possible accuracy for the indirect m_h determination assuming $M_W=80.356\pm 0.006$ GeV and $m_t=175\pm 0.2$ GeV. The widths of the bands indicate the uncertainty in $\alpha(M_Z)$.

The low luminosity needed at $\sqrt{s}\sim 2m_t$ could probably be accumulated without difficulty using a ring optimized for $\sqrt{s}\sim 2M_W$.

An accuracy of $\Delta M_W\sim 6$ MeV achievable at a muon collider would approach the precision level of the current M_Z measurements. It will test the consistency of the standard model at the multiloop level, whatever the Higgs boson mass value is, or probe physics beyond the SM. A low energy muon collider program that explores W^+W^- and $t\bar{t}$ threshold prodcution, s-channel Higgs production [36,37], and Zh threshold production [42], could have enormous impact on SM physics and beyond.

ACKNOWLEDGMENTS

We thank B. Kniehl for providing us with a program to evaluate SM radiative corrections, and D. Zeppenfeld and S. Willenbrock for discussions about the determination of α and the top-quark pole mass. We also thank M. Peskin for a discussion on top-quark threshold physics. This work was supported in part by the U.S. Department of Energy under Grant Nos. DE-FG02-95ER40896, DE-FG03-91ER40674, and DE-FG02-91ER40661. Further support was provided by the University of Wisconsin Research Committee with funds granted by the Wisconsin Alumni Research Foundation, and by the Davis Institute for High Energy Physics.

[1] Proceedings of the First Workshop on the Physics Potential and Development of $\mu^+\mu^-$ Colliders, Napa, California [Nucl. Instrum. Methods Phys. Res. A 350, 24 (1994)].

[2] *Proceedings of the Second Workshop on the Physics Potential and Development of $\mu^+\mu^-$ Colliders*, Sausalito, California, 1994, edited by D. Cline, AIP Conf. Proc. No. 352 (AIP, New York, 1995).

[3] Proceedings of the 9th Advanced ICFA Beam Dynamics Workshop: Beam Dynamics and Technology Issues for $\mu^+\mu^-$ Colliders, Montauk, Long Island, N.Y., 1995 (unpublished).

[4] Proceedings of the Symposium on Physics Potential and Development of $\mu^+\mu^-$ Colliders, San Francisco, California, 1995 (unpublished).

[5] $\mu^+\mu^-$ Collider: A Feasibility Study, Snowmass, Colorado, 1996 (unpublished).

[6] For reviews of precision electroweak physics, see, e.g., W. Hollik, talk given at the 28th International Conference on

High-Energy Physics (ICHEP 96), Warsaw, Poland, Report No. hep-ph/9610457 (unpublished); *Precision Tests of the Standard Electroweak Model*, edited by Paul Langacker (World Scientific, Singapore, 1995).

[7] M. Demarteau, talk given at DPF96, Minneapolis, MN, 1996 (unpublished); B. Winer, talk given at DPF96.

[8] B. Kniehl, Z. Phys. C **72**, 437 (1996).

[9] A. D. Martin and D. Zeppenfeld, Phys. Lett. B **345**, 558 (1995).

[10] P. N. Burrows *et al.*, Report No. SLAC-PUB-7371, hep-ex/9612012, in Proceedings of 1996 DPF/DPB Summer Study on New Directions for High-Energy Physics, Snowmass, CO, 1996 (unpublished).

[11] H. Burkhardt and B. Pietrzyk, Phys. Lett. B **356**, 398 (1995); S. Eidelmann and F. Jegerlehner, Z. Phys. C **67**, 585 (1995); R. B. Nevzorov, A. V. Novikov, and M. I. Vysoitsky, JETP Lett. **60**, 399 (1994); M. Swartz, Phys. Rev. D **53**, 5268 (1996).

[12] D. Zeppenfeld (private communication).

[13] U. Bauer and M. Demarteau *et al.*, Report No. hep-ph/9611334, in Proceedings of 1996 DPF/DPB Summer Study on New Directions for High-Energy Physics, Snowmass, CO, 1996 (unpublished).

[14] S. Keller and J. Womersley, Report No. hep-ph/9611327, in Proceedings of 1996 DPF/DPB Summer Study on New Directions for High-Energy Physics, Snowmass, CO, 1996 (unpublished).

[15] Z. Kunszt *et al.*, in *Proceedings of the Workshop on Physics at LEP 2*, edited by G. Alterelli, T. Sjostrand, and F. Zwirner (CERN Yellow Report No. CERN-96-01, Geneva, Switzerland, 1996), Vol. 1, p. 141, hep-ph/9602352; W. J. Stirling, Nucl. Phys. **B456**, 3 (1995).

[16] A. Miyamoto, in *Proceedings of the Workshop on Physics and Experiments with Linear e^+e^- Colliders*, Waikoloa, Hawaii, 1993, edited by F. A. Harris *et al.* (World Scientific, Singapore, 1993), p. 141.

[17] P. Igo-Kemenes, in *Proceedings of the Workshop on Physics and Experiments with Linear e^+e^- Colliders* [16], p. 95; SLAC Report 485, Physics and Technology of the Next Linear Collider (unpublished).

[18] S. Dawson, Report No. hep-ph/9512250, to appear in Ref. [3].

[19] R. B. Palmer (private communication).

[20] T. Muta, R. Najima, and S. Wakaizumi, Mod. Phys. Lett. A **1**, 203 (1986).

[21] V. S. Fadin, V. A. Khoze, and A. D. Martin, Phys. Lett. B **311**, 311 (1993); V. S. Fadin, V. A. Khoze, A. D. Martin, and W. J. Stirling, *ibid.* **363**, 112 (1995); V. S. Fadin, V. A. Khoze, A. D. Martin, and A. Chapovsky, Phys. Rev. D **52**, 1377 (1995).

[22] Particle Data Group, R. M. Barnett *et al.*, Phys. Rev. D **54**, 1 (1996).

[23] The TeV-2000 Study Group Report, edited by D. Amidei and R. Brock, FERMILAB-Pub/96-082, 1996 (unpublished).

[24] For a recent review on the top-quark physics near the threshold, see, e.g., J. H. Kuhn, TTP-96-18, lectures delivered at SLAC Summer Institute, Stanford, CA, 1995 (unpublished).

[25] V. Barger, M. S. Berger, and P. Ohmann, Phys. Rev. D **47**, 1093 (1993).

[26] V. S. Fadin and V. A. Khoze, JETP Lett. **46**, 525 (1987); Sov. J. Nucl. Phys. **48**, 309 (1988).

[27] J. Feigenbaum, Phys. Rev. D **43**, 264 (1991).

[28] W. Kwong, Phys. Rev. D **43**, 1488 (1991).

[29] M. Strassler and M. Peskin, Phys. Rev. D **43**, 1500 (1991).

[30] M. Jezabek, J. H. Kuhn, and T. Teubner, Z. Phys. C **56**, 653 (1992); M. Jezabek and T. Tuebner, *ibid.* **59**, 669 (1993); M. Jezabek, in *Physics at LEP 200 and Beyond*, Proceedings of the Workshop on Elementary Particle Physics, Teupitz, Germany, 1994, edited by T. Riemann and J. Blumlein [Nucl. Phys. B (Proc. Suppl.) **37B**, (1997)], hep-ph/9406411; M. Jezabek, Acta Phys. Pol. B **26**, 789 (1995); J. H. Kuhn, *ibid.* **26**, 711 (1995).

[31] G. Bagliesi, Workshops on Future e^+e^- Linear Colliders, Hamburg, Germany and Saariselka, Finland, 1991, Report No. CERN-PPE/92-05 (unpublished).

[32] Y. Sumino, K. Fujii, K. Hagiwara, H. Murayama, and C.-K. Ng, Phys. Rev. D **47**, 56 (1993); H. Murayama and Y. Sumino, *ibid.* **47**, 82 (1993); Y. Sumino, Acta Phys. Pol. B **25**, 1837 (1994).

[33] P. Igo-Kemenes, M. Martinez, R. Miquel, and S. Orteu, Contribution to the Workshop on Physics with Linear e^+e^- Colliders at 500 GeV, Report No. CERN-PPE/93-200 (unpublished).

[34] K. Fujii, T. Matsui, and Y. Sumino, Phys. Rev. D **50**, 4341 (1994).

[35] K. Hagiwara, S. Jacobs, M. G. Olsson, and K. J. Miller, Phys. Lett. **130B**, 209 (1983).

[36] V. Barger, M. S. Berger, J. F. Gunion, and T. Han, Phys. Rev. Lett. **75**, 1462 (1995).

[37] V. Barger, M. S. Berger, J. F. Gunion, and T. Han, Report No. CD-96-6, hep-ph/9602415 (unpublished), Phys. Rep. (to be published).

[38] M. Jezabek and J. H. Kuhn, Phys. Lett. B **316**, 360 (1993).

[39] See, e.g., J. Gunion, H. Haber, G. Kane, and S. Dawson, *The Higgs Hunters Guide* (Addison-Wesley, New York, 1990).

[40] A. H. Hoang, Report No. TTP96-19, hep-ph/9606288 (unpublished).

[41] M. C. Smith and S. Willenbrock, Report No. hep-ph/9612329 (unpublished).

[42] V. Barger, M. S. Berger, J. F. Gunion, and T. Han, Phys. Rev. Lett. **79**, 3991 (1997).